Published in final edited form as:
J Vis. ; 8(1): 18.1–1812. doi:10.1167/8.1.18.

Changes in crystalline lens radii of curvature and lens tilt and decentration during dynamic accommodation in rhesus monkeys

Patricia Rosales,
Instituto de Óptica, Consejo Superior de Investigaciones Científicas, Madrid, Spain

Mark Wendt,
University of Houston, College of Optometry, Houston, TX, USA

Susana Marcos, and
Instituto de Óptica, Consejo Superior de Investigaciones Científicas, Madrid, Spain

Adrian Glasser
University of Houston, College of Optometry, Houston, TX, USA

Abstract

Dynamic changes in crystalline lens radii of curvature and lens tilt and decentration were measured during centrally stimulated accommodation in four iridectomized eyes of two adolescent rhesus monkeys. Phakometry measurements were performed dynamically using a custom-built, video-based, Purkinje-image instrument. Lens anterior and posterior radii were calculated from reflections of paired light sources from the ocular surfaces (Purkinje images PI, PIII, and PIV). Lens tilt and decentration were calculated assuming linearity between Purkinje image positions, eye rotation, lens tilt, and decentration. Because the monkey eyes were iridectomized, Purkinje images were referred to the mid-point of the double first Purkinje image (PI). Mean unaccommodated values of anterior and posterior lens radii of curvature were 11.11 ± 1.58 mm and −6.64 ± 0.62 mm, respectively, and these decreased relatively linearly with accommodation in all eyes, at a rate of 0.48 ± 0.14 mm/D and 0.17 ± 0.03 mm/D for anterior and posterior lens surfaces, respectively. Tilt and decentration did not change significantly with accommodation except for tilt around the horizontal axis, which changed at a rate of 0.147 ± 0.25 deg/D. These results are important to fully characterize accommodation in rhesus monkeys.

Keywords

dynamic accommodation; phakometry; tilt; decentration; crystalline; presbyopia

Introduction

Accommodation is an increase in the dioptric power of the eye that enables the image of near objects to be focused on the retina. According to the classic Helmholtz mechanism of accommodation (Von Helmholtz, 1855), during distant vision (when the lens is unaccommodated), the ciliary muscle is relaxed, the zonular fibers are under tension, and the

Corresponding author: Patricia Rosales. Patricia@io.cfmac.csic.es. Address: C/Serrano n- 121, Instituto de Óptica Daza de Valdés (Consejo Superior de Investigaciones Científicas), Madrid, Spain.

Commercial relationships: none.

lens is pulled flat. During accommodation, the ciliary muscle contracts, releasing tension on the zonular fibers at the lens equator, allowing the lens equatorial diameter to decrease, the lens thickness to increase, and the lens anterior surface to become more steeply curved.

The study of biometric changes of the crystalline lens and ciliary body during dynamic accommodation is essential to understand the mechanism of accommodation and age-related changes leading to presbyopia. The lenticular accommodative biometric data most widely available refer to axial changes in the anterior segment. Anterior movement of the anterior crystalline lens surface and an increase in lens thickness has been demonstrated in several studies, in both humans (Beers & van der Heijde, 1994; Bolz, Prinz, Drexler, & Findl, 2007; Dubbelman, van der Heijde, & Weeber, 2001; Fincham, 1925; Garner & Yap, 1997; Ostrin, Kasthurirangan, Win-Hall, & Glasser, 2006; Zadnik, Mutti, & Adams, 1992) and rhesus monkeys either drug stimulated (Koretz, Bertasso, Neider, True-Galbet, & Kaufman, 1987) or centrally stimulated (Vilupuru & Glasser, 2005). Accommodative movement of the posterior lens surface has only recently become clear. Corrected Scheimpflug images show a posterior accommodative movement of the posterior lens surface (Dubbelman, van der Heijde, & Weeber, 2005). Two recent studies in humans related measurements of anterior chamber depth, lens thickness, and anterior segment length using A-scan ultrasonography or partial coherence interferometry with refraction measured simultaneously either in the same eye or in the contralateral eye (Bolz et al., 2007; Ostrin et al., 2006). These studies show a clear posterior accommodative movement of the posterior lens surface. Strikingly similar results occur with centrally stimulated accommodation in rhesus monkeys (Vilupuru & Glasser, 2005). Changes in anterior and/or posterior lens curvature with accommodation in humans have been reported by several authors, using either Purkinje (Cramer, 1853; Garner, 1983; Garner & Smith, 1997; Garner & Yap, 1997; Kirschkamp, Dunne, & Barry, 2004; Von Helmholtz, 1855) or Scheimpflug imaging (Brown, 1973; Dubbelman et al., 2005; Koretz et al., 1987; Koretz, Handelman, & Brown, 1984). A recent study showed comparable results from Purkinje and Scheimpflug methods on the same group of human eyes, both unaccommodated or for different accommodative demands (Rosales, Dubbelman, Marcos, & Van der Heijde, 2006). The use of iridectomized monkeys (Kaufman & Lütjen-Drecoll, 1975) has allowed measurements to be performed on lenticular regions generally not accessible with optical techniques in eyes with intact irides. For example, a decrease in lens equatorial diameter with increased accommodation (Glasser, Wendt, & Ostrin, 2006), as well as centripetal ciliary processes and lens edge movements have been demonstrated dynamically using slit-lamp goniovideography (Croft et al., 2006; Ostrin & Glasser, 2007). While axial changes in lens position, and centripetal movements of the crystalline lens have been studied in detail, to our knowledge only one human study has looked at possible changes in crystalline lens tilt and decentration (in the horizontal direction) for unaccommodated and accommodated eyes (Kirschkamp et al., 2004), for an accommodative demand of 4 D. The change in crystalline lens shape and alignment has implications for the accommodative mechanism and for accommodative optical performance. Optical aberrations have been measured for different accommodative demands in humans, both statically (Cheng et al., 2004; He, Burns, & Marcos, 2000) or dynamically (Hofer, Artal, Singer, Aragón, & Williams, 2001) as well as in enucleated monkey eyes (Roorda & Glasser, 2004) and dynamically in iridectomized centrally stimulated monkeys (Vilupuru, Roorda, & Glasser, 2004). These studies all report a consistent shift of spherical aberration with accommodation toward more negative values (which must be related to changes in the lens shape and/or gradient index distribution). An increase in vertical coma with accommodation is shown in some humans (Cheng et al., 2004; Plainis, Ginis, & Pallikaris, 2005) and monkeys (Vilupuru et al., 2004), suggesting an increase in the lens vertical decentration and/or tilt. Other studies have examined the potential role of monochromatic aberrations on accommodation dynamics (Chen, Kruger, Hofer, Singer, & Williams, 2006; Fernández & Artal, 2005; Radhakrishnan & Charman, 2007).

In the present study, ocular biometry and infrared photorefraction were measured dynamically during Edinger–Westphal (EW)-stimulated accommodation in anesthetized, iridectomized rhesus monkeys for identical stimulus current amplitudes. Changes in anterior and posterior crystalline lens radii, lens tilt, and decentration were also measured dynamically for the same stimulus amplitudes using a custom-built phakometry Purkinje imaging technique. Phakometry has been validated previously (Rosales & Marcos, 2006) and cross validated with Scheimpflug imaging for unaccommodated eyes and as a function of accommodation (Rosales et al., 2006) as well as for measurements of lens tilt and decentration (de Castro, Rosales, & Marcos, 2007). Those measurements, together with biometric and photorefractive measurements in monkey eyes (Vilupuru & Glasser, 2005), are useful to fully characterize the accommodative mechanism in a widely accepted animal model for human accommodation and presbyopia (Glasser & Kaufman, 1999; Glasser et al., 2006; Koretz et al., 1987). Fully characterizing the accommodative mechanism is essential to understand the progression of presbyopia and to aid in strategies to correct presbyopia, i.e., for the design of accommodative intraocular lenses (Küchle et al., 2004; Stachs, Schneider, Stave, & Guthoff, 2005), lens refilling (Koopmans et al., 2006; Norrby, Koopmans, & Terwee, 2006), laser or chemical treatment of the lens (Krueger, Seiler, Gruchman, Mrochen, & Berlin, 2001; Myers & Krueger, 1998), or other surgical procedures (Qazi, Pepose, & Shuster, 2002).

Materials and methods

Animals

The left and right eyes of two anesthetized rhesus monkeys (#54 and #58) were imaged during EW-stimulated accommodation. The monkeys were aged 9 years, 1 month, and 9 years, 3 months, respectively, and had previously undergone complete, bilateral removal of the irides (Kaufman & Lütjen-Drecoll, 1975) and surgical implantation of stimulating electrodes into the EW nucleus (Crawford, Terasawa, & Kaufman 1989). All experiments followed the ARVO Statement for the Use of Animals in Ophthalmic and Vision Research and were performed in accordance with institutionally approved animal protocols.

Measurement of current stimulus/accommodative response

At the start of each experiment, a Hartinger coincidence refractometer (Zeiss, Jena, Germany) was used to measure the static accommodative response for each eye as a function of increasing stimulus amplitudes. Baseline refraction and maximal accommodated refraction achieved at each stimulus amplitude was recorded. Accommodative amplitude at each stimulus current amplitude was the difference between these two refractions.

Dynamic measurement of accommodation

Infrared photorefraction was used to measure dynamic changes in refractive state during centrally stimulated accommodation (Glasser & Kaufman, 1999; Schaeffel, Farkas, & Howland, 1987; Schaeffel, Howland, & Farkas, 1986; Vilupuru & Glasser, 2002). In each experiment, a calibration curve was generated to relate the slope of the vertical brightness profile through the pupil to the absolute refractive state of the eye obtained with the previous Hartinger coincidence refractometer measurements. The dynamic photorefractive optical change occurring in the eye during centrally stimulated accommodation was recorded onto videotape, and subsequent image analysis was performed to measure the pupil brightness profile. The calibration curve was then used to relate the dynamic changes in the pupil brightness profile to the accommodative amplitude.

Dynamic biometric measurements

Biometric changes were measured with continuous high-resolution A-scan ultrasound biometry (CUB) (Beers & van der Heijde, 1994; Vilupuru & Glasser, 2005). Biometric measurements were recorded to a computer at 100 Hz, using a 10-MHz transducer. The transducer contacted the cornea through ultrasound transmission gel to generate sharp A-scan peaks representing the anterior and posterior cornea surfaces, anterior and posterior lens surfaces, and the retina. The CUB measures the time between peaks associated with the intraocular surfaces. These times are converted to distances using standard, accepted sound velocities: anterior and vitreous chambers, 1532 m/s, and lens, 1641 m/s (van der Heijde & Weber, 1989; Vilupuru & Glasser, 2005). Biometric changes were recorded during a sequence of increasing EW-stimulated accommodative responses. The same stimulus current amplitudes used during the photorefraction described earlier were used for the CUB measurements.

Dynamic measurement of phakometry and lens tilt and decentration

A custom-built dynamic (30 Hz) video-based phakometer was used to measure lens radii of curvature and lens tilt and decentration. The set-up included a broad spectrum, white light source, two collimated optic fibers (to assure that the Purkinje images are in focus), and a video camera with a telecentric lens to capture the reflections produced by the anterior cornea (PI) and the anterior and posterior lens surfaces (PIII, PIV). This system was modified from that described previously (Mutti, Zadnik, & Adams, 1992). The collimated light sources used for illumination were adjustable and were separated horizontally between 5 and 10 deg from the optical axis of the camera for the measurements.

Both phakometry and lens tilt and decentration data were calculated from the same measurements using the double light sources. Measurements were performed with a plano profusion speculum lens filled with saline solution placed over the monkey's cornea to effectively neutralize the cornea and improve Purkinje image visibility. This was a custom made lens with an open circular base designed to fit under the eye lids against the conjunctiva concentrically around the limbus. The lens held a 5-ml volume chamber in front of the cornea with a plano clear glass cover slip on the front with an inlet and an outlet tube to fill the chamber in front of the cornea with normal buffered saline (Glasser et al., 2006).

To calculate anterior and posterior lens radii of curvature, the heights of PIII and PIV relative to PI ((h3/h1) and (h4/h1), respectively), were measured frame-by-frame from the recorded video phakometry images. Corneal curvature, measured from a linear calibration curve obtained from calibrating the phakometer on a set of steel calibration ball bearings of different, known radii, and lens thickness and anterior chamber depth measured with A-scan ultrasound biometry, were used in the calculations, using the equivalent mirror theorem (Smith & Garner, 1996) and an iterative method (Garner, 1997) with custom routines written in Matlab (Rosales & Marcos, 2006).

To measure lens tilt and decentration a linear relationship between Purkinje image locations, eye rotation β, lens tilt α, and lens decentration d were assumed according to Phillips' linear equations (Phillips, Pérez-Emmanuelli, Rosskothen, & Koester, 1988). PI = $E\beta$; PIII = $F\beta + C\alpha + Ed$; PIV = $G\beta + D\alpha + Ed$; PI, PIII, and PIV are the relative locations of the midpoint of the double 1st, 3rd, and 4th Purkinje images, and A, B, C, D, E, F, and G are coefficients that depend on the individual ocular biometry. Since the eyes were iridectomized, the pupil center could not be located and therefore be used as a reference for PI, PIII, and PIV. Alternatively, we used the midpoint of the double PI as a reference. Considering that the head was not rotated, and head and eye rotation did not change with accommodation (the first Purkinje image did not move significantly with accommodation, this approximation

should be appropriate). To calculate the coefficients of the Phillips equations, eyes were modeled using Zemax with measured A-scan biometric parameters and lens radii obtained from phakometry measurements. Each of the variables was individually set to zero except one, and the Purkinje image locations were estimated as that one variable's value was changed. The procedure is described in detail previously (Rosales & Marcos, 2006).

To evaluate the validity of these algorithms on a monkey eye with the corneal neutralizing perfusion lens in front of the eye, computer simulations were performed with the lens on the eye. A model eye was built in Zemax with anterior and posterior lens radii of 9.09 mm and −5.93 mm, respectively. The Purkinje images for the monkey eye and the experimental configuration were simulated, and the simulated images were processed with the same algorithms used for processing the real images. Anterior and posterior lens radii were calculated with an accuracy of 0.11 and 0.07 mm, respectively. Similarly, an eye was simulated with nominal values for tilt and decentration of 1 deg and 5 deg for tilt around the vertical axis and tilt around the horizontal axis, and 0.5 mm and 0.1 mm for horizontal and vertical decentration. Tilt and decentration were calculated with an accuracy of 0.089 deg and 0.009 mm, respectively, with respect to the nominal values.

Experimental protocols

Monkeys were initially anesthetized with intramuscular ketamine (10 mg/kg) and acepromazine (0.5 mg/kg). Surgical depth anesthesia was induced with an initial bolus of 1.5 mg/kg followed by constant perfusion at 0.5 mg/kg/min of intravenous propofol (Propoflo, Abbott Laboratories, North Chicago, IL).

The anesthetized monkeys were placed prone with the head held in a head holder, upright and facing forward for all measurements. At the beginning of each experimental session, sutures were tied beneath the medial and lateral rectus muscles of the monkey eye and light tension applied by micrometers to reduce convergent eye movements. The eyelids were held open with lid speculums. A plano polymethylmethacrylate contact lens was placed on the cornea for refraction measurements to maintain optical quality and prevent dehydration. Five, 4-s duration stimulus trains (600-μs pulse duration, 72 Hz, amplitude range 10 to 2,000 μA) with a 4-s interstimulus interval were used to induce varying amplitudes of accommodation. The accommodative response to three different current amplitudes was first measured using a Hartinger coincidence refractometer. The same increasing stimulus amplitudes were used for the same monkey throughout the session. Infrared video photorefraction was performed with a contact lens on the cornea. Video phakometry was then performed, with the corneal neutralizing perfusion speculum. Finally, because it was a contact procedure, A-scan ultrasound biometry was performed with ultrasound transmission gel on the cornea. For monkey #54, one eye was measured per session over approximately 2 hours, 1 month apart. For monkey #58, both eyes were measured in the same session. For each procedure and for each stimulus amplitude, only the last three of the five stimulus trains were analyzed.

Lens tilt and decentration were calculated for the unaccommodated state and accommodative responses for the different current stimuli. Because the tilt and decentration calculations were more computationally demanding, this analysis was not done on the entire dynamic data traces. Instead, a total of 15 images were analyzed from the last three stimuli. Six images were captured when the stimulus was OFF, and 9 images were captured when the stimulus was ON near the end of the stimulus train when the eye was in a stable and maximally accommodated state for each of three different increasing stimulus amplitudes. The images were captured during each of the last three stimuli. The corresponding averaged optical biometry data, for the corresponding stimulation sequences were used for data processing.

Results

EW-stimulated accommodation

Figure 1 shows the Hartinger measured accommodative response for each stimulus current amplitude for the four eyes. These functions were used to convert the stimulus current amplitudes into actual accommodative response for the photorefraction calibration procedures.

Maximum accommodative response amplitudes were 9.91 D for monkey #54 OD, 7.75 for monkey #54 OS, 5.75 D for monkey #58 OD and 9.65 for monkey #58 OS.

In this experiment, the accommodative response for a given current stimulus varied across eyes and between eyes of the same monkey, dependent on the anatomical position of the stimulating electrode.

Dynamic photorefraction and biometry

Photorefraction, anterior chamber depth, and lens thickness were recorded dynamically at 30 Hz. These measurements, along with the dynamic recording of the Purkinje images, allowed dynamic changes in lens curvatures to be calculated. Figure 2 shows an example of dynamic recording of photorefraction and biometry for monkey #54 OS, for one stimulus (off–on–off). The abrupt step trace at the bottom of the graph indicates the start, duration (4 s), and termination of the stimulus train. Anterior chamber depth (ACD) decreases systematically, and lens thickness (LT) increases systematically with accommodation. These dynamic data recorded at 30 Hz were used, along with 30 Hz phakometry images, for calculations of lens radii of curvature and lens tilt and decentration for the same accommodative levels. The repeatability of EW-stimulated accommodative responses has been demonstrated in previous studies (Glasser et al., 2006;Vilupuru & Glasser, 2005), temporal registration of the different measurements is possible to within 1/30 of a second (i.e., at the video frame rate).

Figure 3 shows dynamic biometric changes (anterior chamber depth and lens thickness) with accommodation for all eyes. Data are from the last stimulus producing the maximum accommodative amplitude.

Changes in anterior and posterior lens radii with accommodation

Movie 1 shows a typical phakometry sequence of accommodation and disaccommodation. The distances of the double PIII and PIV (relative to PI) were measured for each video frame and used along with the corresponding optical biometry values to calculate the anterior and posterior lens radii dynamically. Figure 4 shows an example of changes in anterior and posterior lens radii of curvature for monkey #54 OS for the same stimulus sequence as shown in Figure 2.

Average unaccommodated anterior and posterior lens radii were 11.11 ± 1.58 mm and −6.64 ± 0.62 mm, respectively, and decrease (in absolute values) systematically with accommodation in all eyes (Figure 5). Average values were obtained from the last three of the five stimuli applied. For the same accommodative level, there are individual differences in the anterior and posterior radii of curvatures. The amounts and rate of change tend to be similar across eyes of the same monkey. Anterior and posterior lens radii decreased on average by 3.25 mm and 1.14 mm, respectively, between 0 to 6 D of accommodation. Radii decreased at a rate of 0.48 ± 0.14 mm/D and 0.17 ± 0.03 mm/D for anterior and posterior lens surfaces, respectively.

A better comparison of the rate of decrease in radii of curvature across eyes can be performed by relating all values to the unaccommodated state. Figure 6 shows average

changes in radii of curvature as a function of accommodation, relative to the unaccommodated state, averaged across eyes. Since the accommodative responses differed across eyes, spline fitting to the data was performed to average across the individual data from each eye. The curves in Figure 6 show similar slopes for the anterior and posterior surface (0.0058 mm^{-1}/D and 0.0056 mm^{-1}/D, respectively, averaging across eyes and monkeys), indicating that both surfaces contribute similarly to change in power. The curves are relatively linear for the first 4 D, indicating that the relative contribution of the surfaces to the lens power change is rather constant with accommodation.

Changes in lens tilt and decentration with accommodation

The tilt and decentration nomenclature and sign conventions are illustrated in Figure 7. Positive tilt around the horizontal axis (α_x) means that superior edge of the lens moves closer to the cornea than the inferior edge, and vice versa for negative. Positive tilt around the vertical axis (α_y) means that the nasal edge of the right lens or the temporal edge of the left lens moves backward, and vice versa for negative.

Positive horizontal decentration (d_x) means that the right lens is shifted toward the nasal side or that the left lens is shifted towards the temporal side and vice versa for negative. Positive vertical decentration (d_y) indicates that the lens is shifted upwards and vice versa for negative.

Tables 1a and 1b show measurements of tilt and decentration (horizontal and vertical components) for each eye.

Average unaccommodated lens tilt around the vertical axis was 5.69 ± 3.31 deg, and average tilt around the horizontal axis was −0.69 ± 0.93 deg. Average unaccommodated lens decentration was 0.10 ± 0.11 mm horizontally and 0.82 ± 0.20 mm vertically. With accommodation, tilt around the horizontal axis increases significantly ($p < 0.0044$) for all eyes except for #54 OD. The largest increase occurred for eye #58 OS, for which tilt around the horizontal axis increased at a rate of 0.39 deg/D (a total increase of 3.77 deg between 0 and 9.7 D of accommodation). Tilts around the vertical axis were much smaller than tilts around the horizontal axis. Decentration did not change significantly with accommodation in any of the eyes.

Discussion

Dynamic accommodative measurements of the anterior and posterior lens radii of curvature and lens tilt and decentration have been presented for the first time in monkey eyes. These measurements are important to fully characterize the accommodative mechanism in rhesus monkey eyes. Comparisons of the ocular changes measured here during accommodation in monkeys with those measured in humans will further serve to test the extent of the similarity. This study was primarily directed at measuring lens radius, tilt, and decentration and how they change during accommodation. For the unaccommodated state, average anterior lens radius of 11.11 ± 1.58 mm and posterior lens radius of −6.64 ± 0.62 mm were found from the four eyes of the two monkeys. These values are close to the values reported for a four-surface schematic eye of macaque monkey obtained by an optical method (Lapuerta & Schein, 1995). Results obtained here for the anterior and posterior lens radii in monkeys using a collimated light source were not significantly different between the equivalent mirror theorem and the merit function. In previous studies (Rosales et al., 2006; Rosales & Marcos, 2006), a difference between the two algorithms was found, very likely due to the use of an uncollimated light source. An accommodative change in monkeys of −0.48 ± 0.14 mm/D and 0.17 ± 0.03 mm/D for the anterior and posterior lens radii of curvature were found using a Purkinje imaging method in the present study. In terms of

changes of curvature per diopter of accommodation, those slopes would be 0.006 mm^{-1}/D and 0.00485 mm^{-1}/D for the anterior and posterior lens, respectively. A prior study using drug-stimulated accommodation in monkey eyes found approximately −0.272 mm/D and 0.215 mm/D for the anterior and posterior lens using Scheimpflug imaging in two eyes of one monkey (Koretz et al., 1987).

Changes in lens radii of curvature with accommodation in human eyes differ across studies. Some studies found changes in the human eye which are close to the results of the present study in monkey eyes. For example, Koretz, Cook, and Kaufman (2002), using Scheimpflug on one 19-year-old human subject found a mean change of −0.33 mm/D and 0.15 mm/D for the anterior and posterior lens radii of curvature, respectively. However, while most studies report similar changes for the posterior lens, in general larger changes are measured for the anterior lens in humans than those found in the present study for monkeys. Garner and Yap (1997), using Purkinje imaging, found a value of −0.62 mm/D and 0.17 mm/D for anterior and posterior lens radii on average in a group of 11 young eyes (21.2 ± 2.6 years). Dubbelman et al. (2005), also using Scheimpflug imaging, found changes of −0.62 mm/D and 0.13 mm/D for anterior and posterior lens radius, respectively (0.0067 mm^{-1}/D and 0.0037 mm^{-1}/D in terms of curvature). Differences across studies are not necessarily associated with the technique (Scheimpflug or Purkinje imaging). In a recent study, similar values for anterior and posterior lens radii of curvature with accommodative effort were found using Scheimpflug (−0.64 ± 0.04 and 0.23 ± 0.08 mm/D for the anterior and posterior lens radius, respectively) or Purkinje imaging (−0.57 ± 0.05 and 0.29 ± 0.04 mm/D for the anterior and posterior lens radius) on the same human eyes (mean age: 28.5) (Rosales et al., 2006). The fact that most previous human studies relate phakometry measurements to accommodative demand rather than to the actual accommodative response cannot be the cause for the discrepancy, since compensation for the accommodative lag would increase the relative mm/D accommodative changes of the radii of curvature rather than decrease them. Although a direct comparison between results obtained from monkey and human eyes cannot be done due to differences in eye size and different experimental protocols (contralateral accommodation; pharmacological, natural, or centrally stimulated accommodation or differences in the ages of the subjects), the results presented here suggest that change in anterior radius of curvature per diopter of accommodation is lower in iridectomized monkeys than in human eyes, indicating than other factors (i.e., gradient index distribution or lens surface asphericity) may play a role in the change of lens power with accommodation. When the unaccommodated radii of curvature and the accommodative change in lens curvatures for 10 D of accommodation found in the present study are applied to a monkey schematic eye (Lapuerta & Schein, 1995) using the Bennett–Rabbets schematic eye model (Bennett & Rabbetts, 1984), with a uniform equivalent refractive index lens, this accounts for only 7.8 D of accommodation. If a gradient refractive index (GRIN) model was used, the reported differences in lens radii of curvature between monkeys and humans would be even larger and would result in a relatively larger contribution of GRIN to the crystalline lens power change with accommodation in monkeys than in humans.

Some authors have attributed a role of the iris to modify the shape of the anterior lens with increased accommodation (McWhae & Reimer, 2000). However, the absence of iris in the monkeys in this study cannot be the cause of any differences between humans and monkeys. It has been shown that removal of the iris does not affect the EW-stimulated accommodative amplitude in monkeys (Crawford, Kaufman, & Bito, 1990). Further, in the present study, the optical accommodative response, as well as the accommodative biometric changes, was actually measured, so the calculated changes in curvature were related to the actual accommodative change in refraction, lens thickness and anterior chamber depth that occurred.

A factor that may produce an underestimation of lens radii of curvature is the fact that primate lenses are in fact aspherical surfaces. The influence of asphericity on the Purkinje estimates of lens radii was analyzed in depth in a previous study (Rosales et al., 2006). This study found that, particularly for the anterior surface, asphericity had a minimal influence on the lens radius estimates. However, in the previous study, the lens area was limited by the pupil and therefore probably closer to the apical region. In the iridectomized monkey eyes, where no constraints are imposed by the iris, the Purkinje images were reflected off more peripheral regions of the lens where the asphericity may be more of a factor.

The values obtained for tilt and decentration in this study on monkeys are larger than those found in prior studies in humans. In a previous study (Rosales & Marcos, 2006), average tilt and decentrations in young (26.67 ± 2.31 years old on average) human eyes for the unaccommodated state were 1.05 ± 1.12 deg and 0.77 ± 1.27 deg for tilt around the vertical axis and tilt around the horizontal axis, respectively, and 0.28 ± 0.8 mm and −0.06 ± 0.08 mm for horizontal and vertical decentration, respectively. Part of the differences may be due to a systematic accommodative decentration of the pupil center (used as a reference in the previous study) with respect to the midpoint of the first double Purkinje image (used as a reference in the present study, due to the absence of the pupil in the iridectomized eye). Pupil decentration affects both the reference for decentration, as well as the reference axis for tilt (which was the pupillary axis in previous studies). In the monkey experiments, the eye did not converge during accommodation. Therefore, while the absolute values of tilt and decentration are likely affected by the choice of reference axis, the relative changes of lens tilt and decentration with accommodation are not. The relative changes of decentration and tilt with accommodation were systematic except for one monkey eye and higher for tilt around the horizontal axis than tilt around the vertical axis and decentration. To our knowledge, the only report of lens tilt and decentration in human eyes for unaccommodated versus accommodated states was unable to find statistical differences (Kirschkamp et al., 2004). Data in that study were only for the horizontal meridian, for an accommodative demand of 4 D.

Lens tilt and decentration can have an effect on ocular aberrations. In a previous study, it was shown that the amounts of tilt and decentration present in human eyes, particularly in eyes with intraocular lenses, have a very small impact on image quality (Barbero, Marcos, & Jiménez-Alfaro, 2003; Rosales & Marcos, 2007). In human eyes, asymmetric aberrations (such as coma) do not change systematically with accommodation (He et al., 2000), although one study reports minor changes of coma in some subjects, particularly in the vertical direction (Plainis et al., 2005). Also, previous observations in monkeys during centrally stimulated accommodation are consistent with significant changes in lens tilt and decentration, particularly in the vertical direction (Glasser & Kaufman, 1999). The greater tilt of the lens around the horizontal axis reported in the present study is consistent with the observation that gravity influences the movement of the crystalline lens during accommodation in monkeys (Glasser & Kaufman, 1999). Also the change in tilt with accommodation may affect high order aberrations, particularly coma. Vertical coma has been shown to increase significantly and systematically with increasing accommodation compared to the unaccommodated state in some centrally stimulated iridectomized monkey eyes (Vilupuru et al., 2004). Changes in horizontal coma were not significant (Glasser, personal communication), which is supported by the small amounts of tilt around the vertical axis and horizontal decentration found in the present study. Customized computer eye modeling shows that lens tilt tends to compensate the optical effects produced by eye rotation (Rosales & Marcos, 2007). It is certainly possible that the tension induced with sutures to minimize accommodative convergent eye movements as used in this study may impact the tilt and decentration results reported here. Also, the systematic changes in tilt that appear to occur with EW-stimulated accommodation in at least some anesthetized rhesus

monkeys may stem from several factors. EW stimulation may produce greater contractions of the ciliary muscle than could occur with voluntary accommodation. The rhesus monkey ciliary muscle may be capable of far greater accommodative excursions than the human ciliary muscle. EW-stimulated accommodation in young rhesus monkeys can produce 15 D or more of accommodation, whereas 10 D is nearing the upper limit of voluntary accommodation in young humans. Further, the presence of the iris, especially when constricted during accommodation, may provide greater stability to the lens than in iridectomized eyes.

In conclusion, dynamic phakometry, tilt, and decentration were measured for the first time in monkey eyes during accommodation using Purkinje imaging. Changes in the lens radii of curvature with accommodation are consistent with those found in human eyes, with the anterior lens getting steeper at a faster rate. Tilt, particularly around the horizontal axis, changed significantly with accommodation in some eyes, apparently more than in human eyes. No significant changes in lens decentration were found. The differences may be attributable to interspecies variations, age differences, and experimental manipulations. These results are important to fully characterize the accommodation mechanism in monkey eyes, to understand the age changes that occur in the accommodative mechanism, as well as for the evaluation and design of strategies for presbyopia correction, for example, lens refilling (for which the relative contribution of lens curvature and refractive index is critical).

Acknowledgments

This research was supported by National Institutes of Health Grant # RO1 EY014651 (AG), Ministerio de Educación y Ciencia, Spain grant # FIS2005-04382 (SM) and predoctoral fellowship # BFM2002-02638 (PR), and EuroHORCs-European Science Foundation EURYI Award (SM). Thanks to Rob van der Heijde for the CUB, to Siddharth Poonja for the CUB software, and to Chris Kuether for building the neutralizing perfusion speculum lens.

References

Barbero S, Marcos S, Jiménez-Alfaro I. Optical aberrations of intraocular lenses measured in vivo and in vitro. Journal of the Optical Society of America A, Optics, Image Science, and Vision 2003;20:1841–1851.

Beers AP, van der Heijde GL. In vivo determination of the biomechanical properties of the component elements of the accommodation mechanism. Vision Research 1994;34:2897–2905. [PubMed: 7975324]

Bennett, AG.; Rabbetts, RB. Clinical visual optics. 1. London, UK: Butterworths; 1984.

Bolz M, Prinz A, Drexler W, Findl O. Linear relationship of refractive and biometric lenticular changes during accommodation in emmetropic and myopic eyes. British Journal of Ophthalmology 2007;91:360–365. [PubMed: 17050582]

Brown N. Slit-image photography and measurement of the eye. Medical and Biological Illustration 1973;23:192–203.

Chen L, Kruger PB, Hofer H, Singer B, Williams DR. Accommodation with higher-order monochromatic aberrations corrected with adaptive optics. Journal of the Optical Society of America A, Optics, Image Science, and Vision 2006;23:1–8.

Cheng, H.; Barnett, JK.; Vilupuru, AS.; Marsack, JD.; Kasthurirangan, S.; Applegate, RA., et al. A population study on changes in wave aberrations with accommodation; Journal of Vision. 2004. p. 3p. 272-280.http://journalofvision.org/4/4/3/

Cramer, A. Het accommodatievermogen der oogen physiologisch toegelicht. Haarlem: De Erven Loosjes; 1853. p. 35-37.

Crawford KS, Kaufman PL, Bito LZ. The role of the iris in accommodation of rhesus monkeys. Investigative Ophthalmology & Visual Science 1990;31:2185–2190. [PubMed: 2211015]

Crawford K, Terasawa E, Kaufman PL. Reproducible stimulation of ciliary muscle contraction in the cynomolgus monkey via a permanent indwelling midbrain electrode. Brain Research 1989;503:265–272. [PubMed: 2605519]

Croft MA, Glasser A, Heatley G, McDonald J, Ebbert T, Nadkarni NV, et al. The zonula, lens, and circumlental space in the normal iridectomized rhesus monkey eye. Investigative Ophthalmology & Visual Science 2006;47:1087–1095. [PubMed: 16505045]

de Castro A, Rosales P, Marcos S. Tilt and decentration of intraocular lenses in vivo from Purkinje and Scheimpflug imaging. Validation study. Journal of Cataract and Refractive Surgery 2007;33:418–429. [PubMed: 17321392]

Dubbelman M, van der Heijde GL, Weeber HA. The thickness of the aging human lens obtained from corrected Scheimpflug images. Optometry and Vision Science 2001;78:411–416. [PubMed: 11444630]

Dubbelman M, van der Heijde GL, Weeber HA. Change in shape of the aging human crystalline lens with accommodation. Vision Research 2005;45:117–132. [PubMed: 15571742]

Fernández EJ, Artal P. Study on the effects of monochromatic aberrations in the accommodation response by using adaptive optics. Journal of the Optical Society of America A, Optics, Image Science, and Vision 2005;22:1732–1738.

Fincham EF. The changes in the form of the crystalline lens in accommodation. Transactions of the Ophthalmological Society 1925;26:239–269.

Garner LF. Mechanisms of accommodation and refractive error. Ophthalmic & Physiological Optics 1983;3:287–293. [PubMed: 6646763]

Garner LF. Calculation of the radii of curvature of the crystalline lens surfaces. Ophthalmic & Physiological Optics 1997;17:75–80. [PubMed: 9135816]

Garner LF, Smith G. Changes in equivalent and gradient refractive index of the crystalline lens with accommodation. Optometry and Vision Science 1997;74:114–119. [PubMed: 9097329]

Garner LF, Yap MK. Changes in ocular dimensions and refraction with accommodation. Ophthalmic & Physiological Optics 1997;17:12–17. [PubMed: 9135807]

Glasser A, Kaufman PL. The mechanism of accommodation in primates. Ophthalmology 1999;106:863–872. [PubMed: 10328382]

Glasser A, Wendt M, Ostrin L. Accommodative changes in lens diameter in rhesus monkeys. Investigative Ophthalmology & Visual Science 2006;47:278–286. [PubMed: 16384974]

He JC, Burns SA, Marcos S. Monochromatic aberrations in the accommodated human eye. Vision Research 2000;40:41–48. [PubMed: 10768040]

Hofer H, Artal P, Singer B, Aragón J, Williams D. Dynamics of the eye's wave aberration. Journal of the Optical Society of America A, Optics, Image Science, and Vision 2001;18:497–506.

Kaufman PL, Lütjen-Drecoll E. Total iridectomy in the primate in vivo: Surgical technique and postoperative anatomy. Investigative Ophthalmology 1975;14:766–771. [PubMed: 810452]

Kirschkamp T, Dunne M, Barry JC. Phakometric measurement of ocular surface radii of curvature, axial separations and alignment in relaxed and accommodated human eyes. Ophthalmic & Physiological Optics 2004;24:65–73. [PubMed: 15005670]

Koopmans SA, Terwee T, Glasser A, Wendt M, Vilupuru AS, van Kooten TG, et al. Accommodative lens refilling in rhesus monkeys. Investigative Ophthalmology & Visual Science 2006;47:2976–2984. [PubMed: 16799042]

Koretz JF, Bertasso AM, Neider MW, True-Galbelt BA, Kaufman PL. Slit-lamp studies of the rhesus monkey eye: II. Changes in crystalline lens shape, thickness and position during accommodation and aging. Experimental Eye Research 1987;45:317–326. [PubMed: 3653294]

Koretz JF, Cook C, Kaufman PL. Aging of the human lens: Changes in lens shape upon accommodation and with accommodative loss. Journal of the Optical Society of America A, Optics, Image Science, and Vision 2002;19:144–151.

Koretz JF, Handelman GH, Brown NP. Analysis of human crystalline lens curvature as a function of accommodative stage and age. Vision Research 1984;24:1141–1151. [PubMed: 6523736]

Krueger RR, Seiler T, Gruchman T, Mrochen M, Berlin MS. Stress wave amplitudes during laser surgery of the cornea. Ophthalmology 2001;108:1070–1074. [PubMed: 11382631]

Küchle M, Seitz B, Langenbucher A, Gusek-Schneider GC, Martus P, Nguyen NX, et al. Comparison of 6-month results of implantation of the 1CU accommodative intraocular lens with conventional intraocular lenses. Ophthalmology 2004;111:318–124. [PubMed: 15019382]

Lapuerta P, Schein SJ. A four-surface schematic eye of macaque monkey obtained by an optical method. Vision Research 1995;35:2245–2254. [PubMed: 7571461]

McWhae JA, Reimer J. The mechanism of accommodation in primates. Ophthalmology 2000;107:627–628. [PubMed: 10768322]

Mutti DO, Zadnik K, Adams AJ. A video technique for phakometry of the human crystalline lens. Investigative Ophthalmology & Visual Science 1992;33:1771–1782. [PubMed: 1559777]

Myers RI, Krueger RR. Novel approaches to correction of presbyopia with laser modification of the crystalline lens. Journal of Refractive Surgery 1998;14:136–139. [PubMed: 9574744]

Norrby S, Koopmans S, Terwee T. Artificial crystalline lens. Ophthalmology Clinics of North America 2006;19:143–146. [PubMed: 16500536]

Ostrin LA, Glasser A. Edinger–Westphal and pharmacologically stimulated accommodative refractive changes and lens ciliary process movements in rhesus monkeys. Experimental Eye Research 2007;84:302–313. [PubMed: 17137577]

Ostrin LA, Kasthurirangan S, Win-Hall D, Glasser A. Simultaneous measurements of refraction and A-scan biometry during accommodation in humans. Optometry and Vision Science 2006;83:657–665. [PubMed: 16971844]

Phillips P, Pérez-Emmanuelli J, Rosskothen HD, Koester CJ. Measurement of intraocular lens decentration and tilt in vivo. Journal of Cataract and Refractive Surgery 1988;14:129–135. [PubMed: 3351748]

Plainis, S.; Ginis, HS.; Pallikaris, A. The effect of ocular aberrations on steady-state errors of accommodative response; Journal of Vision. 2005. p. 7p. 466-477.http://journalofvision.org/5/5/7/

Qazi MA, Pepose JS, Shuster JJ. Implantation of scleral expansion band segments for the treatment of presbyopia. American Journal of Ophthalmology 2002;134:808–815. [PubMed: 12470747]

Radhakrishnan H, Charman WN. Changes in astigmatism with accommodation. Ophthalmic & Physiological Optics 2007;27:275–280. [PubMed: 17470240]

Roorda, A.; Glasser, A. Wave aberrations of the isolated crystalline lens; Journal of Vision. 2004. p. 1p. 250-261.http://journalofvision.org/4/4/1/

Rosales, P.; Dubbelman, M.; Marcos, S.; Van der Heijde, GL. Crystalline lens radii of curvature from Purkinje and Scheimpflug imaging; Journal of Vision. 2006. p. 5p. 1057-1067.http://journalofvision.org/6/10/5/

Rosales P, Marcos S. Phakometry and lens tilt and decentration using a custom-developed Purkinje imaging apparatus: Validation and measurements. Journal of the Optical Society of America, Optics, Image Science, and Vision 2006;23:509–520.

Rosales P, Marcos S. Customized computer models of eyes with intraocular lenses. Optics Express 2007;15:2204–2218. [PubMed: 19532456]

Schaeffel F, Farkas L, Howland HC. Infrared photoretinoscope. Applied Optics 1987;26:1505–1509. [PubMed: 20454351]

Schaeffel F, Howland HC, Farkas L. Natural accommodation in the growing chicken. Vision Research 1986;26:1977–1993. [PubMed: 3617538]

Smith G, Garner LF. Determination of the radius of curvature of the anterior lens surface from the Purkinje images. Ophthalmic & Physiological Optics 1996;16:135–143. [PubMed: 8762775]

Stachs O, Schneider H, Stave J, Guthoff R. Potentially accommodating intraocular lenses—An in vitro and in vivo study using three-dimensional high-frequency ultrasound. Journal of Refractive Surgery 2005;21:321–323. [PubMed: 16128327]

van der Heijde GL, Weber J. Accommodation used to determine ultrasound velocity in the human lens. Optometry and Vision Science 1989;66:830–833. [PubMed: 2626248]

Vilupuru A, Glasser A. Dynamic accommodation in rhesus monkeys. Vision Research 2002;42:125–141. [PubMed: 11804637]

Vilupuru A, Glasser A. The relationship between refractive and biometric changes during Edinger–Westphal stimulated accommodation in rhesus monkeys. Experimental Eye Research 2005;80:349–360. [PubMed: 15721617]

Vilupuru, A.; Roorda, A.; Glasser, A. Spatially variant changes in lens power during ocular accommodation in a rhesus monkey eye; Journal of Vision. 2004. p. 6p. 299-309.http://journalofvision.org/4/4/6/

Von Helmholtz H. Über die akkommodation des auges. Albrecht von Graefes Archiv für Ophthalmologie 1855;1:1–74.

Zadnik K, Mutti DO, Adams AJ. The repeatability of measurement of the ocular components. Investigative Ophthalmology & Visual Science 1992;33:2325–2333. [PubMed: 1607244]

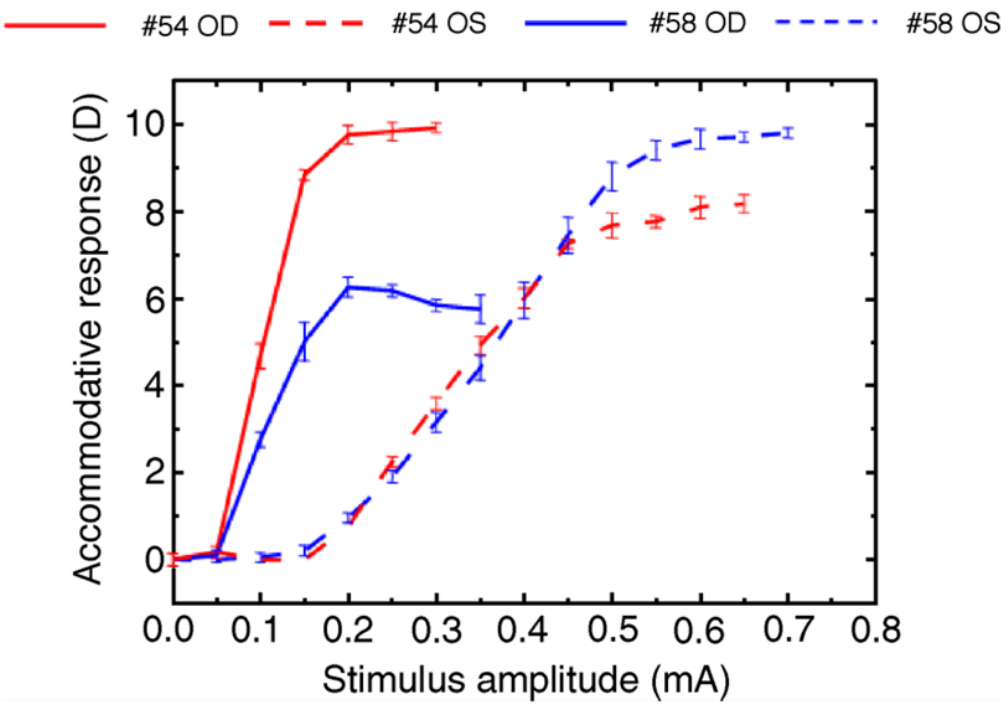

Figure 1.
Accommodative response for each current stimulus for the four eyes of the two monkeys used in this experiment. Each point is the average of three measurements. Error bars are standard deviations.

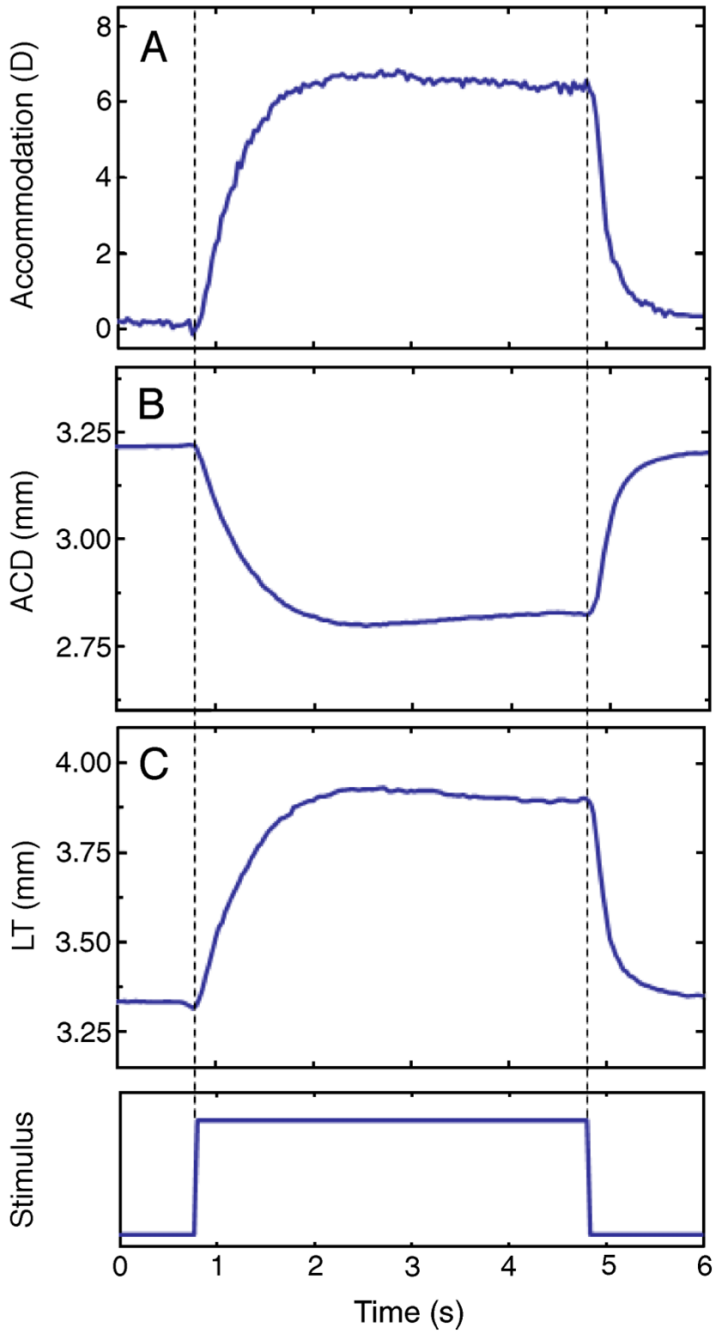

Figure 2.
Dynamic recordings of accommodation from photo-refraction and lens thickness (LT) and anterior chamber depth (ACD) from continuous ultrasound biometry (CUB) from monkey #54 OS, for an accommodation response of 7.75D. Photorefraction was measured first, followed by the CUB measurements for the same stimulus amplitude. This example corresponds to a single response (the 5th response to five, 4-s long stimuli).

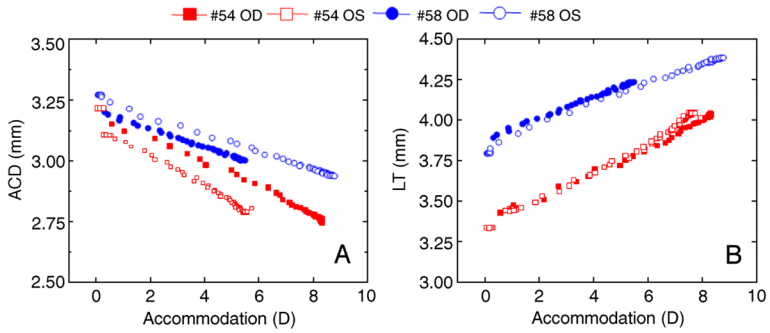

Figure 3.

Dynamic biometric changes (anterior chamber depth and lens thickness) with accommodation for all eyes. Data are from the last stimulus producing the maximum response with accommodation recorded first with photorefraction and ACD and LT recorded subsequently with the CUB.

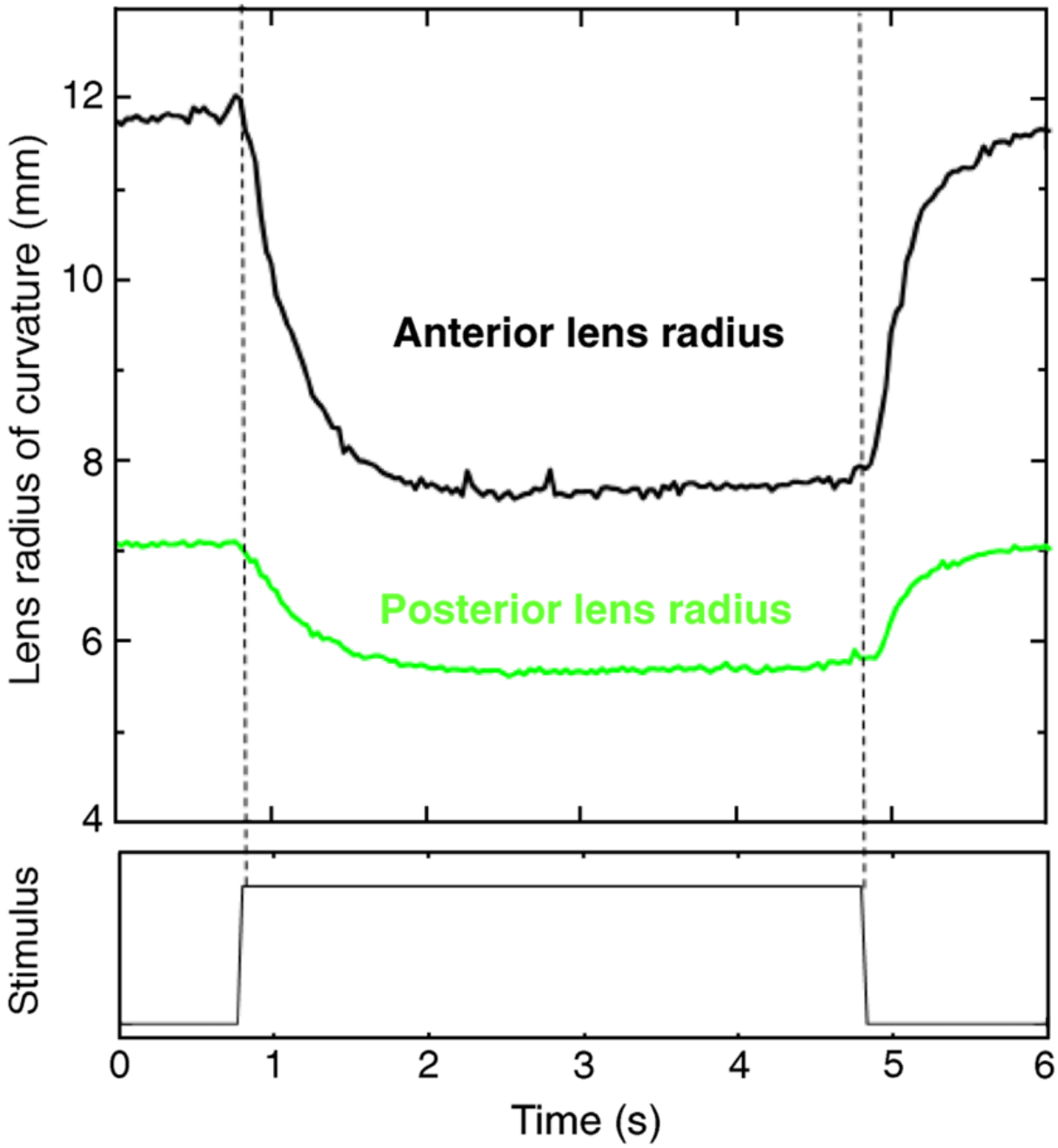

Figure 4.
Change in anterior and posterior lens radii of curvature as a function of accommodation, for a phakometry sequence (5th stimulus). Phakometry data were calculated using individual biometry data shown in Figure 2, for monkey #54 OS.

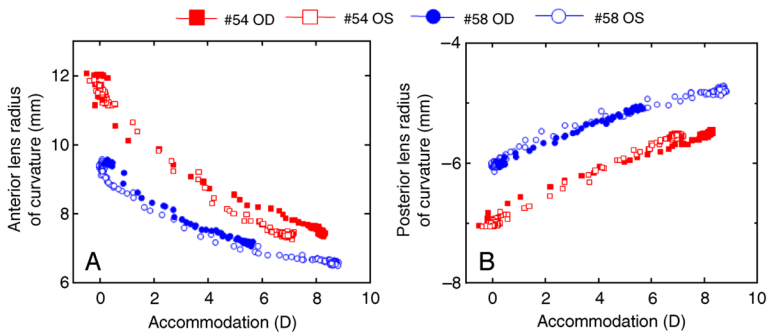

Figure 5.

Anterior and posterior lens radii of curvature as a function of accommodation for both eyes each of monkey #54 and monkey #58. Data are from the 5th stimulus for the maximum accommodative response in the phakometry sequence. Biometry and photorefraction data from each individual eye, corresponding to that shown in Figure 2, were used in the data processing.

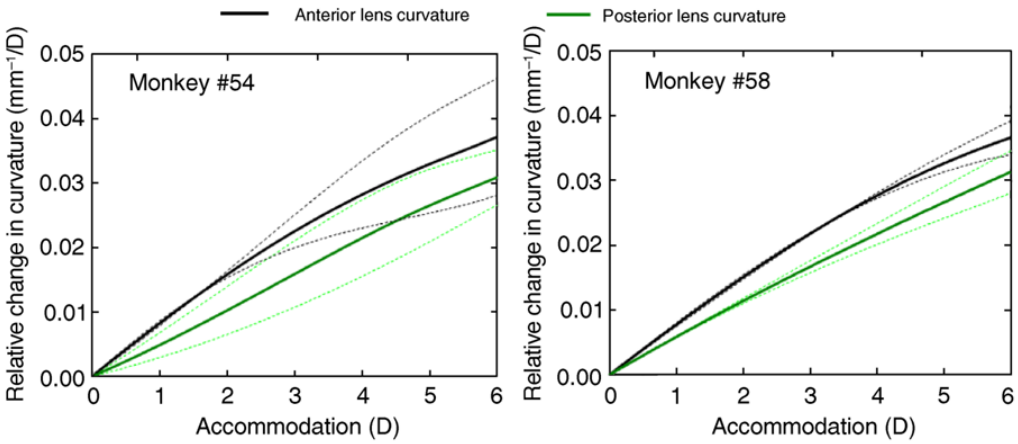

Figure 6.

Average changes in anterior and posterior lens curvatures relative to the un-accommodated state from the two monkeys. Data for each eye were fitted using a spline function and were then averaged across eyes for each monkey at different accommodation levels. Dashed lines represent ±1 standard deviation.

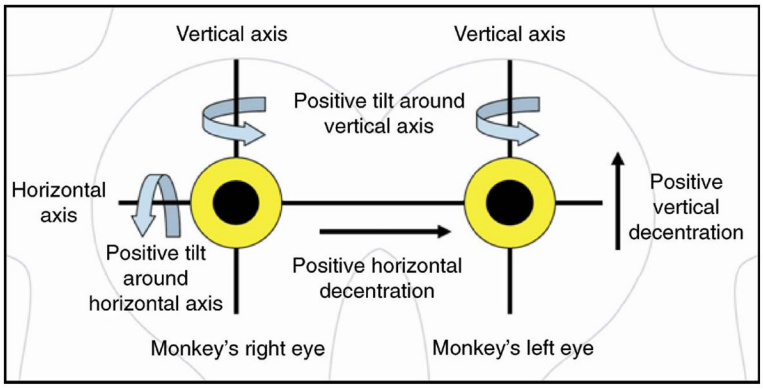

Figure 7.
Nomenclature and sign conventions for lens tilt and decentration, looking into the monkeys eyes, as seen by the observer.

Movie 1.

Phakometry video sequence of changes in the “height” of double Purkinje images PIII (bottom) and PIV (top), with accommodation. The “height” of PI (middle) does not change as the corneal curvature does not change with accommodation. Note that the lens diameter can be seen to decrease with accommodation in the iridectomized eye as the lens surface curvatures become steeper. This sequence is from monkey #54 OS, Stimulus 4, 0.55 mA (accommodation 7.75 D). Phakometry was performed with a fluid interface in front of the eye to neutralize the cornea.

Table 1a

Lens tilt (α in degrees) and decentration (d in mm) for 0 D of accommodation for all eyes.

	α_x	α_y	d_x	d_y
#54 OD	8.97 ± 0.03	−1.09 ± 0.03	0.17 ± 0.01	1 ± 0.01
#54 OS	8.08 ± 0.04	−1.81 ± 0.04	0.17 ± 0.01	0.56 ± 0
#58 OD	3.22 ± 0.06	0.25 ± 0.05	−0.05 ± 0.01	0.95 ± 0.01
#58 OS	2.48 ± 0.05	−0.13 ± 0.15	0.13 ± 0.02	0.79 ± 0.01

Table 1b

Lens tilt (α in degrees) and decentration (d in mm) for the maximum accommodation amplitude for all eyes.

	α_x	α_y	d_x	d_y
#54 OD	9.63 ± 0.11	−1.3 ± 0.12	0.18 ± 0.02	0.94 ± 0.02
#54 OS	6.69 ± 0.2	−0.99 ± 0.12	0.04 ± 0.01	0.44 ± 0.02
#58 OD	5.08 ± 0.15	0.73 ± 0.12	−0.07 ± 0.02	1.03 ± 0.02
#58 OS	6.24 ± 0.18	−1.03 ± 0.13	0.11 ± 0.02	0.92 ± 0.01